Autonomous propulsion of carbon nanotubes powered by a multienzyme ensemble†

Davide Pantarotto, Wesley R. Browne and Ben L. Feringa*

Received (in Cambridge, UK) 5th October 2007, Accepted 8th November 2007
First published as an Advance Article on the web 16th November 2007
DOI: 10.1039/b715310d

Covalent attachment of the enzymes glucose oxidase and catalase to carbon nanotubes enables the tandem catalytic conversion of glucose and H_2O_2 formed to power autonomous movement of the nanotubes.

From intracellular transport and cell division to muscle contraction, nature's protein-based molecular motors[1] serve as a constant source of inspiration to scientists in developing both biohybrid[2–5] and wholly synthetic nano-devices[6–11] powered by light[12–15] and chemical fuels.[16–19] The chemical fuel dihydrogen peroxide has proven to be exceptionally versatile in powering microscopic motion;[20–25] however, for this fuel to be applied successfully, efficient conversion of chemical energy in a controlled manner is essential to achieve motion at the level seen in nature's use of ATP. Bimetallic[20–23,25] and molecular[24] systems have been employed to drive objects of μm dimension using dioxygen bubbles or concentration gradients formed by the catalytic disproportionation of H_2O_2. However, with H_2O_2, its inherent reactivity limits its application in practical devices where such controlled energy release is required.

Here we describe a biohybrid system comprising enzyme functionalized carbon nanotubes that show autonomous translational movement. Covalent attachment of the enzymes glucose oxidase and catalase to carbon nanotubes enables the tandem catalytic conversion of the ubiquitous natural fuel glucose to kinetic energy. Acting in concert, remarkably, these two enzymes produce gaseous molecular dioxygen to propel nanoobjects—rather than the anticipated mechanism involving dioxygen depletion—and provide exciting opportunities towards both autonomous nanoscale transport within biological microenvironments and in exploring the behaviour of complex multienzyme ensembles.

In our approach, *in situ* generation and rapid consumption of the H_2O_2 fuel from the relatively stable and ubiquitous biomolecule β-D-glucose through enzymatic activation of dioxygen provides an attractive alternative to the direct use of H_2O_2 as fuel. For the basic structure of the biohybrid propulsion system (Fig. 1) we chose multi-walled carbon nanotubes (MWCNTs), taking advantage of their peculiar aspect ratio and shape and the methods developed recently for their covalent functionalization.[26–33] Furthermore, MWCNTs functionalized with biomolecules are attractive targets with potential application as cellular delivery vehicles.[30–33] Water solubilization, by oxidation under strongly acidic conditions to introduce carboxylic acid groups at the periphery, of commercial MWCNTs (diameter 20–80 nm, length 0.5–5 μm)[29,34] and purification was followed by analysis and structural characterization using transmission and scanning electron (TEM, SEM) and atomic force (AFM) microscopic techniques (see ESI†). The enzymes were coupled to the carboxylic acid functionalized MWCNTs in aqueous solution using the coupling reagent 1-ethyl-3-(3-dimethylaminopropyl)-carbodiimide (EDC) in a phosphate buffer solution (PBS).

Three different conjugates were prepared (see ESI for details†): **1** GOx functionalized MWCNTs; **2** catalase functionalized MWCNTs; **3** GOx–catalase functionalized MWCNTs. The individual enzymes were coupled in conjugates **1** and **2** as controls and in order to assess their structural and functional integrity and stability when attached covalently to MWCNTs. The loading of each enzyme onto the external surface of the nanotubes was calculated both from assaying enzymatic activity and from the unreacted enzyme remaining after the coupling reaction (see ESI†). For compound **1** an average loading of 296 μg of catalase per mg of nanotubes was determined, whereas for **2**, 680 μg of GOx per mg of nanotubes was found. The average enzyme coverage for compound **3** was fixed at 50% each of the previous values for the individual enzymes. For conjugate **3** a decrease in water

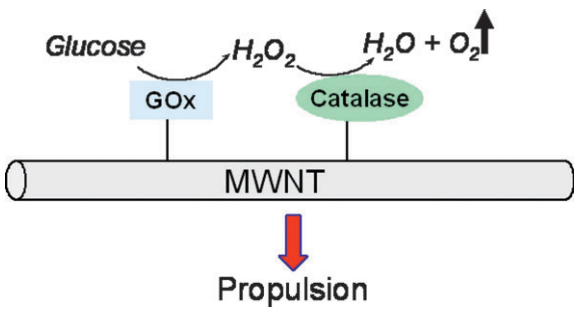

Fig. 1 A biohybrid propulsion system based on the enzymes glucose oxidase (GOx) and catalase, immobilized covalently to water-soluble MWCNTs bearing carboxyl functionalities. The conversion of glucose by GOx produces dihydrogen peroxide, which is decomposed by catalase to generate dioxygen gas bubbles which propel the MWCNTs.

Department of Organic Chemistry, Stratingh Institute for Chemistry and Zernike Institute for Advanced Materials, University of Groningen, Nijenborgh 4, 9747 AG Groningen, The Netherlands. E-mail: b.l.feringa@rug.nl; Fax: +31-503634278; Tel: +31-503634296

† Electronic supplementary information (ESI) available: Synthesis and characterization of **1–3**, experimental details and video files showing movement of nanotubes in the presence of oxygen. See DOI: 10.1039/b715310d

solubility was observed (<1 mg ml^{-1}) compared to **1** (stable colloidal suspension 3.2 mg ml^{-1}) and **2** (stable colloidal suspension 4.4 mg ml^{-1}). Aggregates of **3** featuring large linear or spherical bundles ranging from 10–150 μm in length were observed by optical microscopy (see ESI†). Therefore more dilute aqueous solutions of **3** (typically 100 μg ml^{-1}) were used for TEM, SEM and AFM imaging (Figs. 2 and 3).

Comparison of SEM images of oxidized MWCNTs (Fig. 2A) and conjugate **3** (Fig. 2B), after sputtering with a thin layer of Pt, revealed the coverage of the external surface of the nanotubes with the enzymes. Several grains are present on the surface and analysis of the grain size showed homogeneous enzyme coverage. AFM analysis established the length of the MWCNTs prior to and after attachment of both enzymes (as in **3**) as well as the presence of the enzymes on the walls as can be seen in Fig. 2C,D. Fourier-transform infrared spectroscopic analysis of **1** and **2** verified that only a slight modification in secondary structure (α-helix and β-sheet) of the enzymes is induced upon grafting to the MWCNT surface if compared with the free enzyme (see ESI†).

Analysis of TEM images of **3** reveals the coverage of the external surface of a carbon nanotube by the two enzymes in detail (Fig. 3). In this case negative staining with uranyl acetate was necessary to visualize the biomolecules. From the heterogeneous distribution at the end section of the tube and the dimensions (range 15–30 nm) (Fig. 3, inset), it is reasonable to conclude that several enzyme units are present in each enzyme aggregate.

Optical microscopy enables demonstration of autonomous movement and the effectiveness of the propulsion system due to the concerted action of the two enzymes present in **3**. When a sample of **3** was dispersed in an aqueous phosphate buffered solution at pH 6.8 on a glass cover-slip, with a continuous air flow over the liquid film (sufficiently gentle so as to maintain a stable oxygen concentration in solution while not disturbing the thin film of liquid), in the presence of glucose (100 mM),

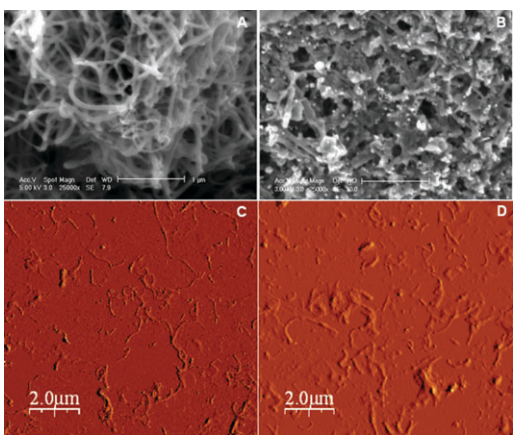

Fig. 2 SEM and AFM images of nanotubes before and after attachment of enzymes. SEM images of: (A) oxidized MWNT (diameter 30 nm) and (B) conjugate **3** (diameter 85 nm due to the presence of the enzyme) after Pt treatment. Bar caption 1 μm. AFM analysis of: (C) oxidized MWNT and (D) conjugate **3** on a flat silicon surface. Average lengths of 1.1 μm and 0.97 μm were measured for C and D, respectively. The edges of the tubes (D) are ill-defined due to the presence of the enzymes.

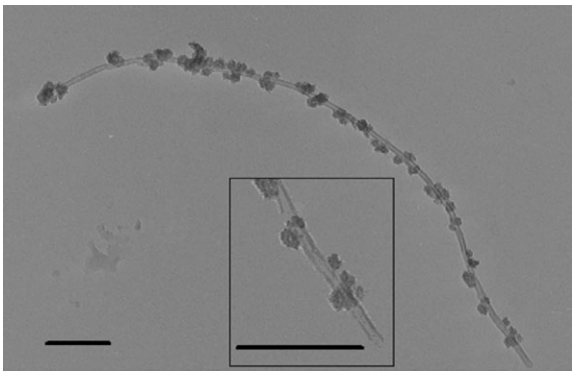

Fig. 3 Microscope image of carbon nanotube with enzymes attached. TEM image of conjugate **3**. The image was recorded at 100 kV after negative staining with uranyl acetate. The MWCNT analyzed has an outer diameter of 20 nm. Globular enzymatic particles have variable dimensions (diameter 15–30 nm), suggesting additional aggregation phenomena. The slow drying process of the specimen can induce further aggregation of the biomolecules on the nanotubes. The inset shows the distribution of the enzyme on the end part of the tube. Bar caption 200 nm.

within a few seconds gentle bubbling of oxygen was observed. The generation of oxygen bubbles induced a translational motion of the small aggregates and bundles of functionalized MWCNTs **3** in the thin liquid film (Fig. 4A, see also video 1, ESI†).

A number of mechanisms for generation of kinetic motion using the catalytic decomposition of H_2O_2 have been proposed, including the generation of oxygen concentration gradients and oxygen bubble formation.[20–25] In the present system overall the oxidation of glucose by GOx and subsequent disproportionation of H_2O_2 by catalase leads to a depletion in the local oxygen concentration and hence movement driven by oxygen concentration gradients would be anticipated. Remarkably, the co-immobilization of the GOx and catalase enzymes, in mixed enzyme assemblies, enables the formation of transiently high oxygen concentrations allowing for oxygen bubble formation and, through this, movement of the nanotube objects.

Depletion of oxygen in solution (*i.e.*, by halting the continuous flow of air) results eventually in a decrease in the movement of **3** and a decrease in the size of the bubbles

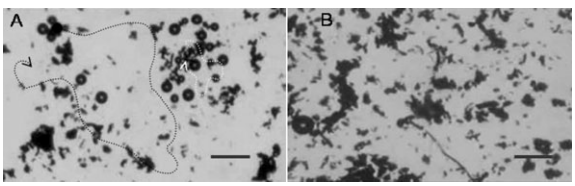

Fig. 4 Effect of exclusion of oxygen on autonomous movement. Observation by video-microscopy of conjugate **3** after addition of a glucose (100 mM) solution under constant air flow (A). The MWCNTs aggregates are visible as black irregular shapes. Bubbles generated from the aggregate are visible as spherical objects. The trajectories of autonomous movement of small aggregates of **3** are shown (see video 1, ESI). When air flow is stopped (B), the rate of bubble formation is reduced. In this case larger aggregates are observed. Bar caption 50 μm.

formed. GOx converts glucose into gluconolactone with molecular oxygen producing dihydrogen peroxide. Therefore oxygen is required to sustain the conversion of glucose by GOx. When catalase is present the H_2O_2 is disproportionated into water and dioxygen with the formation of dioxygen bubbles. Bubble formation is preferred rather than dissolution of the dioxygen produced into the aqueous phase followed by consumption in subsequent GOx enzymatic cycles. The presence of the continuous flow of air or pure dioxygen over the sample maintains the overall concentration of dioxygen in the solution and hence the conversion of glucose. In accordance with this rationale, a similar experiment with **3** under a pure nitrogen flow over the film led to a complete cessation of the bubble formation and the motion was limited, driven only by the less efficient production of gluconolactone and water. It appears that most of the oxygen produced remains dissolved and/or is consumed again by GOx.

Control experiments show that neither **1** nor **2** can engage in the same autonomous motion observed for **3**. The difference in motility between **3**, containing the enzyme propulsion system, and the corresponding non-functionalized MWCNTs is exemplified further in experiments where mixtures of both types of MWCNTs were examined (videos 1 and 2, see ESI†). Furthermore, aggregates of **3** in thin solvent films show that translational movement induced by liquid flow or effects due to temperature dependent Brownian motion is not significant with these nanometre size (200–800 nm) functionalized MWCNT aggregates. The bundles and aggregates of **3**, upon addition of glucose, were propelled at a speed of approximately 0.2–0.8 cm s^{-1} with the speed decreasing over several minutes in accordance with the depletion of glucose in solution, thereby reducing enzymatic conversion, and leading to a cessation of oxygen bubble formation (Fig. 4A, see also video 1, ESI†). However, analysis of the movement of much smaller MWCNT bundles (<100 nm) shows liquid flow and Brownian motion contribute significantly to the dynamic behaviour of **3** (video 3, see ESI†).

Whereas the autonomous movement achieved with **3** is chaotic, the trajectory in the liquid phase appears to be dependent strictly on the shape of the aggregate as well as the position of the enzymes on the MWCNTs. With the present system all our observations point to a propulsion mechanism resulting from local oxygen bubble formation. These results indicate that directionality might be introduced into these systems by controlling the shape of the aggregates formed and by topological control of the coverage of the nanotube by the enzymes.[33,34] As discussed above, this is a remarkable observation as in solution the non-concerted action of GOx and catalase would act to deplete the concentration of molecular oxygen in solution. The approach taken here demonstrates that when held in proximity the kinetic behaviour of mixed enzyme ensembles can surprise us and achieve functions which are thermodynamically unexpected. These preliminary observations will not only guide efforts to control directionality in these autonomously moving carbon nanotubes but offer fascinating opportunities in exploring the behaviour of complex multienzyme ensembles that are otherwise inaccessible *ex-vivo*.

The authors thank the NanoNed consortium and The Netherlands Organisation for Scientific Research (NWO-CW) for financial support.

Notes and references

1 *Molecular Motors*, ed. M. Schliwa, Wiley-VCH, Weinheim, 2003.
2 H. Hess, G. D. Bachand and V. Vogel, *Chem.–Eur. J.*, 2004, **10**, 2110.
3 H. Hess and G. D. Bachand, *Nanotoday*, 2005, **8**, 22.
4 K. Kinbara and T. Aida, *Chem. Rev.*, 2005, **105**, 1377.
5 M. G. L. van den Heuvel and C. Dekker, *Science*, 2007, **317**, 333.
6 W. R. Browne and B. L. Feringa, *Nat. Nanotechnol.*, 2006, **1**, 25.
7 V. Balzani, M. Venturi and A. Credi, *Molecular Devices and Machines: A Journey in the Nano World*, Wiley-VCH, Weinheim, 2003.
8 R. A. L. Jones, *Soft Machines, Nanotechnology and Life*, Oxford University Press, Oxford, 2004.
9 A. R. Pease, J. O. Jeppesen, J. F. Stoddart, Y. Luo, C. P. Collier and J. R. Heath, *Acc. Chem. Res.*, 2001, **34**, 433.
10 J.-P. Sauvage, *Molecular Machines and Motors*, Springer, Berlin, 2001.
11 E. R. Kay, D. A. Leigh and F. Zerbetto, *Angew. Chem., Int. Ed.*, 2007, **46**, 72.
12 N. Koumura, R. W. J. Zijlstra, R. A. van Delden, N. Harada and B. L. Feringa, *Nature*, 1999, **401**, 152.
13 R. A. van Delden, M. K. J. ter Wiel, M. M. Pollard, J. Vicario, N. Koumura and B. L. Feringa, *Nature*, 2005, **437**, 1337.
14 R. Eelkema, M. M. Pollard, J. Vicario, N. Katsonis, B. S. Ramon, C. W. M. Bastiaansen, D. J. Broer and B. L. Feringa, *Nature*, 2006, **440**, 163.
15 S. Saha and J. F. Stoddart, *Chem. Soc. Rev.*, 2007, **36**, 77.
16 T. R. Kelly, H. De Silva and R. A. Silva, *Nature*, 1999, **401**, 150.
17 D. A. Leigh, J. K. Y. Wong, F. Dehez and F. Zerbetto, *Nature*, 2003, **424**, 174.
18 S. P. Fletcher, F. Dumur, M. M. Pollard and B. L. Feringa, *Science*, 2005, **310**, 80.
19 P. L. Anelli, N. Spencer and J. F. Stoddart, *J. Am. Chem. Soc.*, 1991, **113**, 5131.
20 R. F. Ismagilov, A. Schwartz, N. Bowden and G. M. Whitesides, *Angew. Chem., Int. Ed.*, 2002, **41**, 652.
21 T. R. Kline, W. F. Paxton, T. E. Mallouk and A. Sen, *Angew. Chem., Int. Ed.*, 2005, **44**, 744.
22 J. M. Catchmark, S. Subramanian and A. Sen, *Small*, 2005, **1**, 202.
23 S. Fornier-Bidoz, A. C. Arsenault, I. Manners and G. A. Ozin, *Chem. Commun.*, 2005, 441.
24 J. Vicario, R. Eelkema, W. R. Browne, A. Meetsma, R. M. La Crois and B. L. Feringa, *Chem. Commun.*, 2005, 3936.
25 Y. Wang, R. M. Hernandez, D. J. Bartlett, J. M. Bingham, T. R. Kline, A. Sen and T. E. Mallouk, *Langmuir*, 2006, **22**, 10451.
26 J. Chen, M. A. Hamon, H. Hu, Y. S. Chen, A. M. Rao, P. C. Eklund and R. C. Haddon, *Science*, 1998, **282**, 95.
27 J. Liu, A. G. Rinzler, H. J. Dai, J. H. Hafner, R. K. Bradley, P. J. Boul, A. Lu, T. Iverson, K. Shelimov, C. B. Huffman, F. Rodriguez-Macias, Y. S. Shon, T. R. Lee, D. T. Colbert and R. E. Smalley, *Science*, 1998, **280**, 1253.
28 R. C. Haddon, *Acc. Chem. Res.*, 2002, **35**, 997.
29 I. D. Rosca, F. Watari, M. Uo and T. Akasaka, *Carbon*, 2005, **43**, 3124.
30 N. Mano and A. Heller, *J. Am. Chem. Soc.*, 2005, **127**, 11574.
31 D. Cui, *J. Nanosci. Nanotechnol.*, 2007, **7**, 1298.
32 K. Kostarelos, L. Lacerda, G. Pastorin, W. Wu, S. Wieckowski, J. Luangsivilay, S. Godefroy, D. Pantarotto, J. P. Briand, S. Muller, M. Prato and A. Bianco, *Nat. Nanotechnol.*, 2007, **2**, 108.
33 D. Tasis, N. Tagmatarchis, A. Bianco and M. Prato, *Chem. Rev.*, 2006, **106**, 1105.
34 H. Dumortier, S. Lacotte, G. Pastorin, R. Marega, W. Wu, D. Bonifazi, J.-P. Briand, M. Prato, S. Muller and A. Bianco, *Nano Lett.*, 2006, **6**, 1522.